Photodissociation of HBr/LiF(001): A Quantum Mechanical Model

Tamar Seideman‡
Eloret Institute
Palo Alto, CA 94303

‡ Mailing address: NASA Ames Research Center, Mail Stop 230-3, Moffett Field, California 94035-1000

Abstract

The photodissociation dynamics of HBr adsorbed on a LiF(001) surface is studied using time-independent quantum mechanics. The photodissociation lineshape and the $Br(^2P_{1/2})/Br(^2P_{3/2})$ yield ratio are computed and compared with the corresponding quantities for gas phase photodissociation. The angular distribution of the hydrogen photofragments following excitation of adsorbed HBr is computed and found to agree qualitatively with experimental data [Bourdon and coworkers, J.Chem.Phys. **95**, 1361 (1991)]. The effect of polarization of the photon is illustrated and discussed. We find the field polarization to affect significantly the magnitude of the photodissociation signal but not the angular dependence of the photofragment distribution, in agreement with experiment and in accord with expectations for a strongly aligned adsorbed phase.

1. Introduction

The photochemistry of surface adsorbed molecules contains potentially a wealth of valuable information regarding the orientation, the alignment, and the existence of ordering of the adsorbates, the substrate-adsorbate interaction potential, and in some cases also the surface structure.[1,2] The study of photodissociation reactions of adsorbates is thus of importance for understanding and hence optimizing processes such as laser induced surface processing, heterogeneous catalysis and film growth.[3,4]

Whereas photodissociation of molecules adsorbed on metal surfaces is frequently hindered and complicated by competing processes such as quenching and substrate mediated excitation,[5] photodissociation of molecules adsorbed on insulators is controllable experimentally[6–13] and more amenable to theoretical studies.[13–20]

Polanyi and coworkers, in a series of time-of-flight mass spectrometry experiments, investigated the photodissociation of several species of small molecules adsorbed on clear crystal LiF surfaces.[6–9] Further experiments were carried out by Tabares *et al.*,[10] who probed the photodissociation of CH_3Br/LiF(100), and by Trentelman and coworkers,[11–13] who studied the photodissociation of methyl iodide adsorbed on MgO(100). The experimental work has stimulated several recent theoretical studies.[13–20] Most of the theoretical work employed classical simulations[13–18] although a few quantum mechanical models have been also reported.[19,20] McCarthy and Gerber, using molecular dynamics simulations, studied the photodissociation of ICl/MgO(001)[14] and more recently the photodissociation of CH_3I/MgO(001).[13] Strong correlation was found between the orientational preference of the adsorbed phase and the angular distribution of the photofragments.[13,14] Classical simulations of adsorbate photodissociation were carried out also by Huang and Guo,[15,16] by Watson and coworkers,[17] and by Barclay *et al.*[18] Guo and Schatz[19] and McCarthy *et al.*[20] reported reduced dimensionality quantum mechanical studies of CH_3I[19b] and of IBr[20] adsorbed on a MgO surface. Both groups investigated the effect of the surface on the electronic branching ratio of the atomic photofragments. The classical framework[13–18] has the obvious advantage that motion of the surface atoms can be taken into account, at least within a finite cluster model. Classical simulations, however, treat the photodissociation event as an instantaneous switch from the ground to an excited electronic surface which, in case more than a single excited electronic state is involved, may be followed by a curve crossing prior to dissociation. This sequential picture, although convenient, is misleading. Quantum mechanical calculations, on the other hand, are able to describe accurately the photodissociation dynamics, but cannot take into explicit account motion of the surface atoms (except *via* much simplified models[21]) and hence temperature effects are mostly neglected.[19,20] From these previous studies[6–20] it may be concluded that the presence of the sur-

face can affect the photodissociation dynamics in a variety of *qualitatively* different, *system dependent* ways, and that adsorbate photodissociation experiments contain considerable interesting information that is yet to be explored.

In the present work we study the UV photodissociation of HBr adsorbed on a LiF(001) surface using time-independent quantum mechanics. Several desirable features of HBr/LiF have led to our choice of system. LiF has served as substrate in most of the experimental photochemistry on insulators studies to date[1,6–10] due to its high transparency to UV light and to its chemical stability. In particular, studies[9] of HBr/LiF(001) have shown that the heavy Br atom remains adsorbed to the surface subsequent to the dissociation while the hydrogen photofragment is ejected into the vacuum. Thus, the difficulty of dealing with a double continuum is avoided. Furthermore, the experiments[9] were able to distinguish clearly and *characterize separately* hydrogen photofragments that suffered inelastic collisions with the surface or with coadsorbed molecules and those that suffered no such collisions. The photodissociation lineshape and angular distribution of the *latter* fragments is of prime interest for the present study since they contain direct information regarding the surface effect on the dissociation dynamics, which is not affected by subsequent interactions. Several interesting features of HBr/LiF were noted in previous studies:[9,22,23] The angular distribution of the energetic H atoms, the ones that dissociated with no loss of energy, was found to peak at $\approx 55°$ to the surface normal, being independent of the azimuthal (in the surface plane) angle, while the $Br(^2P_{1/2})/Br(^2P_{3/2})$ yield ratio was found to be the same as that following gas phase photodissociation.[9] Due to the small radius of hydrogen and to the size match of the LiF lattice constant and the equilibrium HBr bond length, HBr/LiF(001) exhibits rather strong electrostatic attraction; Fourier transform IR experiments[22] and classical simulations[23] of the adsorbed phase have shown that the Br atom lies over a Li^+ ion, with the hydrogen atom lying approximately over a neighboring F^- ion, slightly tilted with respect to the surface plane (111°-116° from the surface normal). The photodissociation of HBr/LiF is thus expected to reflect the strong electrostatic attraction and orientational preference of the adsorbed phase.

Classical trajectory studies of the HBr/LiF(001) photodissociation were carried out by Huang and Guo,[15] who reported calculations of the H photofragment angular distribution, and more recently by Barclay *et al.*[18] who emphasized the role of surface photodissociation as a first stage in surface-aligned chemistry.[1,8,9] Nevertheless, in view of the light mass of the hydrogen fragment and the nonadiabatic interaction in the excited HBr manifold, a quantum mechanical study appears warranted.

The goal of the present work is to complement the work of Huang and Guo[15] and Barclay and coworkers[18] by carrying out quantum mechanical calculations of the HBr/LiF(001) photodissociation dynamics. Although the calculations reported

below agree with experimental measurements, the major aim of this study is not so much to reproduce the insightful observations of Bourdon *et al.*,[9] but rather to emphasize additional aspects and possibly point out directions for future research. Our computational method is an extension of a recently proposed time-independent scheme for the calculation of gas phase photodissociation dynamics.[24] The method was shown in Ref. 24 to be particularly efficient when only the total photodissociation cross section is of interest. For practical applications of adsorbate photodissociation, for instance modeling of chemical vapor deposition reactors,[4] this is more often than not the desired quantity. Partial cross sections are required in order to compute the angular distribution and branching ratio of the photofragments, and their calculation is emphasized in the present study.

The next section describes our computational model and details the approximations involved. In Sec. 2a we describe our choice of potential energy surfaces while in Sec 2b we review briefly our technique of computing photodissociation cross sections and suggest a method for calculating the photofragment angular distribution. Section 3 presents and discusses our results; we compute the photodissociation lineshape and the $Br(^2P_{1/2})/Br(^2P_{3/2})$ yield ratio for gas phase HBr and compare the results with the corresponding quantities for surface adsorbed HBr. We compute and compare with experiment[9] the angular distribution of the hydrogen photofragments and discuss our results in terms of the substrate-adsorbate interaction. Finally, we illustrate the role played by the polarization of the light field. Section 4 briefly concludes the paper and points out directions for future theoretical work.

2. Method

The application of quantum mechanics to the study of the complex dynamics involved in the photodissociation of an adsorbate requires invoking approximations. The present model considers the photodissociation of a single molecule, ignoring inelastic collisions of the photofragments with the surface and motion of the surface ions. The first approximation may be justified by the fact that even in the presence of inelastic collisions, their effect can be eliminated from the experimental data,[9] and the second by the observation that surface relaxation plays a relatively minor role in the HBr/LiF photodissociation,[15] at least at the experimentally interesting temperatures (typically 85 K). Since the heavy Br atom travels on dissociation $\approx$ 79 times slower than the hydrogen atom, and was found experimentally to remain adsorbed to the surface after dissociation,[9] its motion is neglected in the present study. In order to reduce further the dimensionality of the problem the hydrogen atom is restricted to move in a plane perpendicular to the surface. It will be the goal of future work to systematically relax the aforementioned assumptions and to examine their validity more quantitatively.

Figure 1 shows schematically the configuration of the initial bound state, based on the IR measurements of Ref. 22, and illustrates our choice of coordinate system. We use spherical polar coordinates with the origin at the Br atom and the polar axis defined to lie along the normal to the surface. In terms of the coordinates of Fig. 1 the system (field free) Hamiltonian is given as

$$H = -\frac{1}{2\mu}\frac{1}{R^2}\frac{\partial}{\partial R}R^2\frac{\partial}{\partial R} - \frac{1}{2\mu R^2}\left(\frac{1}{\sin\gamma}\frac{\partial}{\partial\gamma}\sin\gamma\frac{\partial}{\partial\gamma}\right) + V(R,\gamma) \qquad (1a)$$

where μ is the hydrogen mass and atomic units ($\hbar = 1$) have been used. With the standard choice $\Psi(R,\gamma) = \chi(R,\gamma)/R$ the Schrödinger equation takes the form

$$\left\{E + \frac{1}{2\mu}\frac{\partial^2}{\partial R^2} + \frac{1}{2\mu R^2}\left[(1-x^2)\frac{\partial^2}{\partial x^2} + 2x\frac{\partial}{\partial x}\right] - V(R,x)\right\}\chi(R,x) = 0 \qquad (1b)$$

where $x = \cos\gamma$.

a. Potential Energy

Having neglected motion of the surface ions, we find that the potential energy in Eqs. (1) consists of two terms; the HBr potential energy curves $V_a(R)$ and the substrate-adsorbate interaction $V_{s-a}(R,\gamma)$,

$$V(R,\gamma) = V_a(R) + V_{s-a}(R,\gamma)\,. \qquad (2)$$

Electronic structure studies of gas phase HBr were carried out by Chapman and coworkers,[25] who employed relativistic *ab-initio* theory to compute the ground and

several of the excited HBr electronic states as well as the transition dipole functions coupling the ground state with the excited manifold. The lowest electronic absorption band of HBr extends from $\approx$ 150 nm to $\approx$ 220 nm and peaks around 180 nm.[26] In principle, absorption to three excited electronic states is possible at this energy; the $^3\Pi_1$ and $^1\Pi_1$, which correlate asymptotically with ground state Br atoms [Br($^2P_{3/2}$)] and are coupled with the ground HBr state *via* a perpendicular transition, and the $^3\Pi_{0+}$ state which correlates with excited Br atoms [Br* =Br($^2P_{1/2}$)] and is coupled with the ground state *via* a parallel transition. Chapman *et al.*, confirming earlier calculations by Mulliken,[27] showed however, that the transition dipole function coupling the ground with the $^1\Pi_1$ state is over an order of magnitude larger than those coupling the ground state with the $^3\Pi_1$ and $^3\Pi_{0+}$ states. The experimental detection of $\approx$ 14% excited Br atoms[28] has been attributed to spin-orbit coupling between the initially excited $^1\Pi_1$ and the $^3\Pi_{0+}$.[25] A fourth-excited electronic state, the $^3\Sigma_1$, which correlates with Br($^2P_{3/2}$), is accessible at the relevant energies through nonadiabatic interaction. Nevertheless, since the coupling with this state becomes significant only at much larger H–Br separations[25] its effect on the dissociation dynamics is expected to be small. In the present work we thus restrict attention to three (diabatic) electronic states; the ground ($^1\Sigma_{0+}$) state, the $^1\Pi_1$ state which is coupled with the $^1\Sigma_{0+}$ by the electromagnetic field, and the $^3\Pi_{0+}$ state which is coupled with the $^1\Pi_1$ by spin-orbit interaction. The relevant potential energy curves, following a fit to the data of Ref. 25b, are shown in Fig. 2. We fit the dipole moment function of Chapman *et al.* to the form

$$\mu(R) = D_d \exp\left[-b_d(R - R_d)^2\right] \tag{3}$$

with $D_d = 0.38$ a.u., $b_d = 1.2$ Bohr^{-2} and $R_d = 1.8$ Bohr. A functional form for the spin-orbit coupling potential was derived from analysis of the electronic wavefunctions of Refs. 25. We used the asymmetric form

$$V_{so}(R) = D_c \frac{\exp\left[-b_{c1}(R - R_c)^2\right]}{1 + \exp\left[-b_{c2}(R - R_c)\right]} \tag{4}$$

with $D_c = 3.34 \times 10^{-3}$ a.u., $b_{c1} = 0.3$ Bohr^{-2}, $b_{c2} = 1.5$ Bohr^{-1} and $R_c = 4.5$ Bohr.

The substrate-adsorbate potential V_{s-a} in Eq. (2) consists of two terms: an electrostatic term, denoted V^e_{s-a}, which accounts for the interaction between the electric field generated by the surface ions and the charge distribution of the molecule, and a core term, denoted V^c_{s-a}, which describes the short range repulsion of the closed shells and the long range attractive dispersion interactions. The electrostatic forces can in principle be computed by straightforward summation over the pairwise Coulombic interaction of the lattice ions with the adsorbate. This procedure is, however, very difficult to apply in practice due to the long range of the Coulomb force (in fact the

sum of Coulombic terms is known to be only conditionally convergent). As pointed out by Lennard-Jones and Dent[29] and by Steele,[30] the electrostatic potential Φ generated by a regular lattice of surface ions can be accurately expressed as a rapidly converging Fourier series. For the (001) face of an FCC crystal[30]

$$\Phi(\mathbf{r}) = \frac{4e}{a} \sum_{g_1,g_2}{}' \frac{(-1)^{(g_1+g_2)/2} \exp\left[-\frac{2\pi z'}{a}\sqrt{g_1^2+g_2^2}\right]}{\sqrt{g_1^2+g_2^2}\left\{1+\exp\left[-\pi\sqrt{g_1^2+g_2^2}\right]\right\}} \times \cos\left[2\pi\left(g_1\frac{x}{a}+g_2\frac{y}{a}-\frac{g_1+g_2}{4}\right)\right] \tag{5}$$

where e is the electron charge, a is the lattice constant ($a = 4.03$ Å for LiF) and the prime signifies summation over odd values of g_1 and g_2. x and y in Eq (5) are measured in the surface plane, along the [100] and the [010] crystallographic axes, respectively, and z' denotes distance along the normal to the surface, measured with respect to the positive ion chosen as the origin ($z' = z + R_{\mathrm{Li-Br}}$ in Fig. 1). For many physisorbed systems the adsorbate equilibrium position is sufficiently far from the surface ($z' > a$) that only the leading terms in Eq. (5) ($|g_1| = |g_2| = 1$) contribute significantly to the sum. Since, as mentioned in the introduction, the HBr molecule lies relatively close to the surface, more terms should be included but, as is clear from the exponential z' dependence of $\Phi(\mathbf{r})$, the sum converges rapidly. Following Ref. 23 we model the molecule as a distribution of three collinear point charges with $q_1 = 0.276e$ located at the H atom, $q_2 = -0.444e$ located at the Br atom and $q_3 = 0.168e$ located 1.292 Å from the Br end of the molecule, on the opposite side to the H atom. This choice is not unique;[31] other models, such as a two point dipoles model,[23] are possible and were investigated (*vide infra*). With the above choice the electrostatic substrate-adsorbate interaction is written as

$$V^e_{s-a} = \sum_{k=1}^{3} q_k \Phi(\mathbf{r}_k) \tag{6}$$

and thus depends on the molecular orientation relative to the lattice axes. Since the excited HBr electronic states are repulsive and the molecule dissociates into neutral atoms the electrostatic interaction is omitted from the excited potential energy surfaces.

The core interaction V^c_{s-a}, assumed pairwise additive, can be readily computed by direct summation over the surface ions. Following Refs. 18 and 23 we use a Tang-Toennies form

$$\begin{aligned} V^{TT}(q) &= Ae^{-\beta q} - \sum_{n=3}^{\infty} f_{2n}(q)\frac{C_{2n}}{q^{2n}}, \\ f_{2n}(q) &= 1 - \sum_{k=0}^{2n}\frac{(\beta q)^k}{k!}e^{-\beta q}, \end{aligned} \tag{7}$$

where the first (Born-Mayer) term accounts for the short range repulsion and the second term is a damped dispersion series which is typically truncated after its second term. The various parameters in Eq. (7) are taken from the semi-empirical calculations of Barclay and coworkers.[18]

The substrate-adsorbate interaction potential is shown in Figs. 3 as a function of height above the surface (z') and distance along the [100] direction of the crystal (x). Figure 3a corresponds to the bound state, where corrugation is more pronounced and the electrostatic part of the interaction introduces dependence on the orientation of the molecule. Figure 3b corresponds to atomic (free) hydrogen, where the interaction is periodic in x and considerably less corrugated.

Using Eqs. (2, 4–7) the complete HBr/LiF(001) potential energy is given as

$$\begin{aligned} V_g(R,\gamma) &= V_{^1\Sigma_{0^+}}(R) + V^{e}_{s-a}(R,\gamma) + V^{c,b}_{s-a}(R,\gamma) \\ \mathbf{V}_e(R,\gamma) &= \begin{pmatrix} V_{^1\Pi_1}(R) + V^{c,f}_{s-a}(R,\gamma) & V_{so}(R) \\ V_{so}(R) & V_{^3\Pi_{0^+}}(R) + V^{c,f}_{s-a}(R,\gamma) \end{pmatrix} \end{aligned} \tag{8}$$

where g stands for ground, e stands for excited, and $V^{c,b}_{s-a}$ and $V^{c,f}_{s-a}$ denote, respectively, the core interaction [Eq. (7)] in the bound and in the free states.

b. Photodissociation Dynamics

With the field free Hamiltonian fully specified, the photodissociation cross section may be computed *via* a similar method to that described in Ref. 24. The total cross section

$$\begin{aligned} \sigma_{\mathrm{i}}(\omega) &= \sum_{\mathbf{n},l} \sigma_{\mathbf{n}l,\mathrm{i}}(\omega) \\ &= \left(\frac{4\pi^2\omega}{c}\right) \sum_{\mathbf{n},l} \left| \left\langle \Psi^{-}_{E,\mathbf{n},l} \left| \vec{\mu}\cdot\hat{\varepsilon} \right| \Psi_{\mathrm{i},0} \right\rangle \right|^2 \end{aligned} \tag{9}$$

was written as

$$\begin{aligned} \sigma_{\mathrm{i}}(\omega) &= -\left(\frac{4\pi\omega}{c}\right) \mathrm{Im} \left\langle \Psi_{\mathrm{i},0} \left| \vec{\mu}\cdot\hat{\varepsilon}\, G(E^+)\, \vec{\mu}\cdot\hat{\varepsilon} \right| \Psi_{\mathrm{i},0} \right\rangle \\ &= -\left(\frac{4\pi\omega}{c}\right) \mathrm{Im} \sum_{l,l'} \left\langle \chi_{\mathrm{i}} \left| \mu_{0,l}\, G_{l,l'}(E^+)\, \mu_{l',0} \right| \chi_{\mathrm{i}} \right\rangle \end{aligned} \tag{10}$$

where $\left|\Psi_{\mathrm{i},0}\right\rangle$ is a bound state of the matter Hamiltonian, $\left|\Psi^{-}_{E,\mathbf{n},l}\right\rangle$ is an incoming scattering state of the same Hamiltonian, the indices i and n denote collectively the set of rovibrational quantum numbers, and l is an electronic index. $\vec{\mu}\cdot\hat{\varepsilon}$ in Eq. (9) is the component of the transition dipole moment in the direction of the field, the

ground state wavefunction in Eq. (10) is written as a product of an electronic state and a nuclear state, $\left|\Psi_{\mathrm{i},0}\right\rangle = |0\rangle\,|\chi_{\mathrm{i}}\rangle$, $\mu_{0,l} = \langle 0\,|\,\vec{\mu}\cdot\hat{\epsilon}\,|\,l\rangle$, and $G_{l,l'}(E^+)$ is the matrix element of the outgoing Green's operator

$$G(E^+) = \lim_{\epsilon\to 0}(E + i\epsilon - H)^{-1} \tag{11}$$

in the electronic basis.

While the total photodissociation cross section of Eqs. (9, 10) reflects the short time dynamics, partial cross sections are required in order to compute observables that depend on the long time dynamics, such as the branching ratios and quantum state or angular distributions of the photofragments. Using the Lippmann-Schwinger equation for the scattering states in Eq. (9),[32,33]

$$\begin{aligned}\left|\Psi^-_{E,\mathrm{n},l}\right\rangle &= [1 + G(E^-)V']\left|\Psi^{1\,-}_{E,\mathrm{n},l}\right\rangle \\ &= -iG(E^-)\epsilon\left|\Psi^{1\,-}_{E,\mathrm{n},l}\right\rangle ,\end{aligned} \tag{12}$$

where $\left|\Psi^{1\,-}_{E,\mathrm{n},l}\right\rangle$ are solutions of an approximate Hamiltonian $H_1 = H - V'$, the partial cross section can be expressed formally as[24]

$$\begin{aligned}\sigma_{\mathrm{n}l,\mathrm{i}}(\omega) &= \left(\frac{4\pi^2\omega}{c}\right)\left|\left\langle \Psi^{1\,-}_{E,\mathrm{n},l}\left|\epsilon\, G(E^+)\,\vec{\mu}\cdot\hat{\epsilon}\right|\,\Psi_{\mathrm{i},0}\right\rangle\right|^2 \\ &= \left(\frac{4\pi^2\omega}{c}\right)\left|\sum_{l'}\left\langle \chi^{1\,-}_{E,\mathrm{n},l}\left|\epsilon\, G_{l,l'}(E^+)\,\mu_{l',0}\right|\,\chi_{\mathrm{i}}\right\rangle\right|^2 .\end{aligned} \tag{13}$$

We used absorbing boundary conditions (ABC)[24,34] to obtain a well behaved representation of the Green's operator; thus, the infinitesimal convergence factor ϵ in Eq. (11) was replaced by a coordinate dependent operator $\epsilon(\mathrm{q})$ which is practically zero in the interaction region but becomes sizable outside the physically relevant region of space. A discrete variable representation (DVR)[35] was employed for the nuclear degrees of freedom.

In application of Eqs. (12, 13) to surface photodissociation, the boundary conditions that are to be satisfied by the scattering solutions are clearly different from those appropriate to gas phase photodissociation. We first note that the method takes into exact account energy conserving collisions of the photofragment with the surface (i.e., collisions that do not transfer energy to the surface, resulting in the two high energy peaks in the energy distribution of Ref. 9). This can be seen by expanding the Green's operator in terms of its gas phase analogue $G_a(E^+) = (E+i\epsilon-H_a)^{-1}$ where $H_a = T+V_a$ [see Eq. (2)]. Substituting the expansion in Eq. (10), for example,

$$\begin{aligned}\sigma_{\mathrm{i}}(\omega) = -\left(\frac{4\pi\omega}{c}\right)\mathrm{Im}\Big\{&\langle\,\Psi_\mu\,|\,G_a(E^+)\,|\,\Psi_\mu\,\rangle \\ &+\langle\,\Psi_\mu\,|\,G_a(E^+)\,V_{s-a}\,G_a(E^+)\,|\,\Psi_\mu\,\rangle + \ldots\Big\}\end{aligned} \tag{14}$$

where we denoted $|\Psi_\mu\rangle = \vec{\mu}\cdot\hat{\varepsilon}\left|\Psi_{i,0}\right\rangle$. The first term in Eq. (14), $\mathrm{Im}\langle\Psi_\mu|G_a(E^+)|\Psi_\mu\rangle = -\pi\sum_{\mathbf{n},l}\left|\left\langle\Psi_\mu \mid \Psi^{a\,-}_{E,\mathbf{n},l}\right\rangle\right|^2$, where $\left|\Psi^{a\,-}_{E,\mathbf{n},l}\right\rangle$ are eigenstates of H_a, corresponds to the direct photodissociation. Subsequent terms incorporate the effect of multiple, energy conserving collisions with the surface. This is an essential feature for the present system since, as pointed out in the introduction (and discussed in previous studies[9,22,23]), the HBr molecule is well oriented in the adsorbed phase, with the H atom tilted *toward* the surface and hence redirecting collisions of the photofragments with the surface are expected to play a role.

Below we will be particularly interested in calculation of the photofragments' angular distribution, i.e., the *differential* photodissociation cross section $\sigma(\hat{\mathbf{k}},\omega)$. To that end we first write the Lippmann-Schwinger equation in the coordinate representation as

$$\left\langle \mathrm{R} \mid \Psi^{-}_{E,\hat{\mathbf{k}},l}\right\rangle = \left\langle \mathrm{R} \mid \Psi^{1\,-}_{E,\hat{\mathbf{k}},l}\right\rangle + \int d\mathrm{R}'\, G(E^-;\mathrm{R},\mathrm{R}')\, V'(\mathrm{R}')\left\langle \mathrm{R}' \mid \Psi^{1\,-}_{E,\hat{\mathbf{k}},l}\right\rangle \quad (15)$$

where $\hat{\mathbf{k}}$ is a unit vector in the direction of observation and we indicate explicitly the dependence of the scattering wavefunction on both the magnitude and the direction of k. The right hand side of Eq. (15) vanishes in the crystal ($z \to -\infty$) and takes the standard asymptotic form of a scattering solution[32] at large separation from the surface ($R \to \infty$). In Eq. (15) and below we omit the n index from the scattering waves and confine attention to the case of a single displacement vector (here the H–Br displacement vector R) of interest for the present application. The method is, however, equally applicable to the dissociation of polyatomic adsorbates as will be evident from the discussion below. A simple choice for the zero order solutions are (energy normalized) plane waves,

$$\left\langle \mathrm{R} \mid \Psi^{1\,-}_{E,\hat{\mathbf{k}},l}\right\rangle \approx \left\langle \mathrm{R} \mid \Psi^{0}_{E,\hat{\mathbf{k}},l}\right\rangle = \sqrt{\frac{\mu k_l}{(2\pi)^3}}e^{i\mathbf{k}_l\cdot\mathbf{R}} \quad (16)$$

where $k_l = \sqrt{2\mu(E-V_l^\infty)}$ and V_l^∞ is the asymptotic potential in the lth electronic state. Using the resolution of the plane wave[32]

$$e^{i\mathbf{k}\cdot\mathbf{R}} = 4\pi\sum_{j,m} i^j j_j(kR)Y_{j,m}(\hat{\mathrm{R}})Y^*_{j,m}(\hat{\mathbf{k}})\,, \quad (17)$$

where $j_j(kR)$ are spherical Bessel functions,[36] we obtain

$$\left\langle \mathrm{R} \mid \Psi^{-}_{E,\hat{\mathbf{k}},l}\right\rangle = \sqrt{\frac{2\mu k_l}{\pi}}\sum_{j,m} i^j Y^*_{j,m}(\hat{\mathbf{k}})\Big\{ j_j(k_l R)Y_{j,m}(\hat{\mathrm{R}}) + \int d\mathrm{R}'\, G(E^-;\mathrm{R},\mathrm{R}')\, V(\mathrm{R}')\, j_j(k_l R')Y_{j,m}(\hat{\mathrm{R}}')\Big\} \quad (18)$$

where V' of Eq. (15) has been replaced by the complete interaction V. With the notation

$$\left\langle \mathbf{R} \mid f^0_{k,j,m} \right\rangle \equiv \sqrt{\frac{2\mu k}{\pi}} i^j j_j(kR) Y_{j,m}(\hat{\mathbf{R}}) \tag{19}$$

the scattering state is written as

$$\left| \Psi^-_{E,\hat{\mathbf{k}},l} \right\rangle = \sum_{j,m} Y^*_{j,m}(\hat{\mathbf{k}}) \left[1 + G(E^-)V\right] \left| f^0_{k_l,j,m} \right\rangle \tag{20}$$

and, using Eq (12), the differential photodissociation cross section assumes the form

$$\sigma_{l,\mathrm{i}}(\hat{\mathbf{k}},\omega) = \left(\frac{4\pi^2\omega}{c}\right) \left| \sum_{j,m} Y^*_{j,m}(\hat{\mathbf{k}}) \left\langle f^0_{k_l,j,m} \right| \epsilon G(E^+) \vec{\mu}\cdot\hat{\epsilon} \left| \Psi_{\mathrm{i},0} \right\rangle \right|^2 . \tag{21}$$

We note that $\left| f^0_{k,j,m} \right\rangle$ satisfy Schrödinger's equation in spherical coordinates for $V = 0$, thus

$$\int d\hat{\mathbf{k}}\, \sigma_{l,\mathrm{i}}(\hat{\mathbf{k}},\omega) = \sigma_{l,\mathrm{i}}(\omega)$$

where $\sigma_{l,\mathrm{i}}(\omega)$ is given in Eq. (13) and we used the orthonormality of the spherical harmonics, $\int d\hat{\mathbf{k}}\, Y^*_{j,m}(\hat{\mathbf{k}})\, Y_{j',m'}(\hat{\mathbf{k}}) = \delta_{j,j'}\delta_{m,m'}$. For systems where the initial state is aligned at an angle $\gamma_i < \pi/2$ with respect to the normal, as is the case for the photodissociation of CH_3I,[11-13] for instance, Eq. (21) predicts that the angular distribution of the photofragments will peak at an angle $\theta_k \approx \gamma_i$. The symmetry of the spherical harmonics in Eq. (21) ensures that in systems such as HBr/LiF, where $\gamma_i > \pi/2$ and the photofragments are likely to collide with the surface after dissociation, $\sigma(\theta_k,\omega)$ will peak at an angle close to that expected for specular recoil ($\theta_k \approx \pi - \gamma_i$). Deviation from the specular direction which depends on the degree of surface corrugation, and a certain width which reflects the degree of alignment, are expected.

In practice one would normally replace the plane wave solutions by distorted waves,

$$\left| \Psi^{1\,-}_{E,\hat{\mathbf{k}},l} \right\rangle \approx \left| \Psi^0_{E,\hat{\mathbf{k}},l} \right\rangle + G_1(E^-)V_1 \left| \Psi^0_{E,\hat{\mathbf{k}},l} \right\rangle \tag{22}$$

where the potential has been partitioned as $V = V_1 + V'$ and $G_1(E^-)$ is the Green's operator (modified to include an absorbing potential) corresponding to $H_1 = T + V_1$. Thus

$$\begin{aligned} \left| \Psi^-_{E,\hat{\mathbf{k}},l} \right\rangle &= \left[1 + G(E^-)V'\right] \left| \Psi^{1\,-}_{E,\hat{\mathbf{k}},l} \right\rangle \\ &= -\sum_{j,m} Y^*_{j,m}(\hat{\mathbf{k}})\, G(E^-)\, \epsilon\, G_1(E^-)\, \epsilon \left| f^0_{k_l,j,m} \right\rangle \\ &= -i \sum_{j,m} Y^*_{j,m}(\hat{\mathbf{k}})\, G(E^-)\, \epsilon \left| f^{1\,-}_{k_l,j,m} \right\rangle \end{aligned} \tag{23}$$

where $\left| f^{1\,-}_{k_l,j,m} \right\rangle$ are defined by the last equation. Equation (12) holds regardless of our choice of zero order Hamiltonian, thus $\left| f^{1\,-}_{k_l,j,m} \right\rangle$ can be any (physically acceptable) basis. Below we choose

$$\left\langle \mathbf{R} \mid f^{1\,-}_{k,j,m} \right\rangle = g(R\cos\gamma) \left\langle \mathbf{R} \mid f^{0}_{k,j,m} \right\rangle \tag{24}$$

where $g(z = R\cos\gamma)$ is a cutoff function which vanishes as the wavefunction penetrates into the crystal and approaches 1 elsewhere. For more complicated applications it would be desirable to employ a better zero order basis, for instance by including a part of the physical gas-surface interaction in the distorted Hamiltonian, so as to reduce the computational effort.

3. Results and Discussion

The photodissociation lineshape of gas phase HBr, computed *via* Eq. (10), is shown as a dashed curve in Fig. 4. The overall structure and the peak position agree with the experimental data of Lee and Suto.[26] The percentage yield of excited Br atoms [$Br^* = Br(^2P_{1/2})$], obtained by employing Eq. (13) to compute the partial Br and Br^* photodissociation cross sections, is $\approx$ 15% of the total Br yield. The solid line in Fig. 4 shows the photodissociation lineshape for surface adsorbed HBr. The lineshapes have the same overall structure but the one corresponding to the adsorbed phase is slightly distorted and blue shifted by 2.2 nm. We found the ground state to be stabilized in the presence of the surface by $\approx$ 0.18 eV as compared to the gas phase. (A somewhat smaller energy shift, $\approx$ 0.15 eV, was found with a two dipole model for the electrostatic interaction[23] with a corresponding slightly smaller shift of the photodissociation lineshape.) The stabilization, a significant part of which is due to electrostatic interaction, is related to the adsorption energy of HBr. At a given photon energy the translational energy of the photofragment is thus lower by $\approx$ 0.18 eV from the H–Br relative translational energy following gas phase photodissociation [2.6 eV for the $Br(^2P_{3/2})$ channel and 2.14 eV for the $Br(^2P_{1/2})$ channel]. The decreased translational energy of the H photofragment was found also in the experiments of Bourdon and coworkers[9] and in the classical trajectory simulations of Barclay *et al.*,[18] although the reverse effect was found in the classical work of Ref. 15. Since the photodissociation cross section is proportional to the photon frequency (in the weak field limit) the energy shift of the lineshape is somewhat smaller than the stabilization energy of the ground electronic state. The Br^*/Br yield ratio was found to be unaltered from its gas phase value, as was found also experimentally.[9] This result, however, is to be expected since the form of the coupling potential and the relative position of the excited electronic states in the present model are taken to be the same as in the gas phase.

In Fig. 5 we show the angular distribution of the energetic [$Br(^2P_{3/2})$ channel] hydrogen photofragments following excitation of HBr/LiF(001) at 193 nm. The distribution of H fragments corresponding to the Br^* channel was found to have the same structure but a smaller overall magnitude. As shown in Fig. 5, the distribution peaks at $\approx 56°$ with respect to the surface normal, a *smaller* angle than that expected for specular recoil, i.e., for scattering from a flat surface ($69° \rightarrow 64°$ for an initial orientation of $111° \rightarrow 116°$ with respect to the normal). The effect of surface corrugation is thus to tilt the scattered photofragments *toward* the surface normal. Figure 6 shows the experimental angular distribution of Bourdon and coworkers[9] for three different surface coverages. The peak position of the measured curve ($\approx 55°$) and its structure at large angles are reproduced well by the calculated curve of Fig. 5,

although the latter falls off more rapidly at small angles. This discrepancy may be expected since the model considers a single adsorbed molecule while the experiments were carried out at a finite coverage ($0.2 \rightarrow 1.0$ monolayers). Figure 6 shows clearly that the effect of increased coverage is to increase substantially the small angle wing of the distribution while leaving the large angle contribution practically unaltered. As discussed in Sec. 2 the present calculation, which neglects motion of the surface ions, reflects most realistically the limit of zero temperature, while the experiments of Bourdon *et al.* were carried out at 85 K. It appears, however, that our neglect of surface relaxation is not the reason for the discrepancy between the calculated and the experimental distributions at small angles since the present distribution is similar (although broader) to the calculations of Ref. 18. The latter, based on classical simulations and a single excited electronic state model, considered likewise an isolated adsorbate but allowed for temperature effects.

The angular distribution of the fragments is expected to depend on the adsorbate orientation, the effect of redirecting collisions and the polarization of the field. The adsorbate orientation determines both the direction at which photofragments will hit the surface and the orientation of the transition dipole function with respect to the space fixed frame. The field polarization affects the dissociation probability through the dot product $\vec{\mu}\cdot\hat{\varepsilon}$ in Eqs. (9, 13, 21). The electronic transition under consideration is perpendicular[26] and hence $\vec{\mu}\cdot\hat{\varepsilon} = \mu(R)\hat{\mathrm{e}}\cdot\hat{\varepsilon}$ where $\hat{\mathrm{e}}$ is a unit vector perpendicular to $\hat{\mathrm{R}}$ and $\mu(R)$ is given in Eq. (3). The effect of the initial orientation of the adsorbed phase is contained in the form of the ground state wavefunction, which, in turn, reflects the substrate-adsorbate interaction in the ground electronic state. Simple Franck-Condon type considerations based on Eq. (21) indicate that in the case where the initial state is strongly aligned, $\Psi_{i,0}$ has a large amplitude for a narrow range of γ values which give rise to dominance of certain partial waves ($\{j,m\}$). The latter determine the structure of the angular distribution. In that situation the field polarization is expected to affect strongly the *magnitude* of the signal but have little effect on its angular dependence. If, on the other hand, the initial state samples a wide range of orientations, different polarizations will accentuate the contribution of different scattering components and hence alter the form of the angular distribution. Similar conclusions were reached in Ref. 9 based on different considerations. In Fig. 7 we compare the computed angular distributions following dissociation with light polarized along the x and the z axes. As expected, the signal corresponding to x polarized light is considerably smaller than that corresponding to z polarized light (light polarized along the normal to the surface) while the overall structure of the angular distribution is practically invariant to the polarization. Figure 7 is in agreement with polarized light measurements of Bourdon and coworkers[9] who found the angular distribution of the H fragments to be nearly independent of the field

polarization. This result provides an independent support of the finding that the HBr molecule is strongly aligned in the adsorbed phase. A *crude* estimate of the preferred orientation angle may be obtained by comparing the magnitudes of the x and the z polarized light signals. We find $\sigma(\hat{\mathbf{k}},\omega;\hat{\epsilon}=\hat{\mathbf{x}})/\sigma(\hat{\mathbf{k}},\omega;\hat{\epsilon}=\hat{\mathbf{z}}) \approx .38$ indicating a preferred orientation angle of $\gamma_i \approx 111°$ with respect to the normal, in qualitative agreement with experimental IR[22] and photodissociation[9] results, and with molecular dynamics simulations of the adsorbed phase[23] ($\gamma_i \approx 111° - 116°$).

It should be remarked that the structure of the angular distribution depends quite sensitively on the substrate-adsorbate interaction potential, as may be expected in view of the above discussion. Nevertheless, the agreement of our calculated distribution with experiment cannot serve to verify the quantitative details of the potential function of Eqs. (5-7) but only its qualitative features, namely, its corrugated nature and its manner of orienting the initial state.

4. Conclusions

In this work we developed a time-independent, quantum mechanical model for study of adsorbate photodissociation and applied it to the photodissociation of HBr adsorbed on a LiF(001) surface. The photodissociation lineshape of adsorbed HBr was found to be blue shifted with respect to that of the gas phase molecule, consistent with stabilization of the ground electronic state in the presence of the surface. The computed yield ratio of excited Br atoms [$Br^* = Br(^2P_{1/2})$] does not change from its gas phase value according to the present model, as was found also experimentally.[9] The theoretical angular distribution of the H photofragments peaks at $\approx 56°$ to the surface normal in agreement with experiment ($55 \pm 5°$)[9] although the experimental distribution extends to smaller angles. In view of the trend of the experimental distribution with increasing coverage, it is likely that the discrepancy is due to the presence of coadsorbates in the experiment which is not taken into account in our calculations. The role played by the field polarization was examined and discussed. We found the polarization of the electromagnetic field to change significantly the *magnitude* of the signal but not its angular dependence, in agreement with polarized light experiments[9] and in accord with qualitative expectations for a strongly aligned initial state.

As pointed out in the introduction, existing theoretical studies of adsorbate photodissociation can be broadly classified as either purely classical[13–18] or simplified quantum mechanical models.[19,20] The former are able to take into account surface relaxation but treat the photodissociation event and the effect of nonadiabatic coupling in the excited manifold in an approximate manner. The latter, to which the present model belongs, are able to treat accurately the photodissociation process but are forced to neglect motion of the surface ions (or else introduce crude approximations for the interaction). The theory of adsorbate photodissociation therefore appears ideally suited for application of system-bath type approximations[37] where the system degrees of freedom are treated by exact quantum mechanics and the bath modes are approximated. It allows, moreover, a natural separation of the degrees of freedom into an active subspace and a remaining, passive subspace. In particular, like other chemical processes at surfaces, photodissociation reactions of adsorbates have aspects in common with liquid phase processes, where the solvent is treated *statistically*.[38] Doren and Tully[37a] studied the role played by precursor states in adsorption and desorption dynamics using a mean field approach to cast the effect of all modes but the reaction coordinate mode in the form of a temperature-dependent, effective potential for motion along the reaction coordinate. Of the wide variety of system-bath type approximations which have been developed in recent years[37] the approach of Ref. 37a appears most attractive since it introduces a time-independent

effective potential for motion of the system, and since a large number of bath modes can be taken into account. Ideally one would treat statistically only the surface modes, and when applicable, the modes of coadsorbates. Nevertheless variations that include in the bath several of the adsorbate modes are likely to be needed (and valid) in photodissociation studies of larger molecules. Refinement and extension of the present model *via* this and other approaches will be the objective of future research.

Acknowledgments

I am grateful to Dr. D. Schwenke and to Dr. W. Huo for interesting conversations. I would also like to thank Dr. D. Chapman for sending me unpublished data regarding the electronic structure of HBr, and Drs. T. Halicioglu, C. Dateo, and G. Hahne for reading the manuscript. This work was supported by NASA Grant No. NCC2-737.

References

1. For a review of the experimental work prior to 1991 see J.C. Polanyi and H. Rieley, *Photochemistry in the Adsorbed State* in *Dynamics of Gas-Surface Interactions*, edited by C.T. Rettner and M.N.R. Ashfold, The Royal Society of Chemistry, Cambridge, 1991.

2. R. Kosloff and Y. Zeiri, J.Chem.Phys. **97**, 1719 (1992).

3. P.H. Avouris and R.E. Walkup, Annu.Rev.Phys.Chem. **40**, 173 (1989) and references therein.

4. For a review of the experimental aspects of chemical vapor deposition see H. Stafast, App.Phys. **A45**, 96 (1988).

5. N. Ohta, Y. Ohno, and T. Matsushima, Surf.Sci.Lett. **276**, L1 (1992).

6. St. J. Dixon-Warren, I. Harrison, K. Leggett, M.S. Matyjaszczyk, J.C. Polanyi, and P.A. Young, J.Chem.Phys. **88**, 4095 (1988).

7. C-C. Cho, J.C. Polanyi, and C.D. Stanners, J.Chem.Phys. **90**, 598 (1989).

8. I. Harrison, J.C. Polanyi, and P.A. Young, J.Chem.Phys. **89**, 1498 (1988); *ibid*, J.Chem.Phys. **89**, 1475 (1988).

9. E.B.D. Bourdon, C.-C. Cho, P. Das, J.C. Polanyi, C.D. Stanners, and G.-Q. Xu, J.Chem.Phys. **95**, 1361 (1991).

10. F.L. Tabares, E.P. Marsh, G.A. Bach, and J.P. Cowin, J.Chem.Phys. **86**, 738 (1987).

11. K.A. Trentelman, D.H. Fairbrother, P.C. Stair, P.G. Strupp, and E. Weitz, J.Vac.Sci.Techno. **A 9**, 1820 (1991).

12. K.A. Trentelman, D.H. Fairbrother, P.G. Strupp, P.C. Stair, and E. Weitz, J.Chem.Phys. **96**, 9221 (1992).

13. M.I. McCarthy, R.B. Gerber, K.A. Trentelman, P.G. Strupp, D.H. Fairbrother, P.C. Stair, and E. Weitz, J.Chem.Phys. **97**, 5168 (1992).

14. M.I. McCarthy and R.B. Gerber, J.Chem.Phys. **93**, 887 (1990).

15. Z.-H. Huang and H. Guo, J.Chem.Phys. **96**, 8564 (1992).

16. Z.-H. Huang and H. Guo, J.Chem.Phys. **97**, 2110 (1992); *ibid* **98**, 3395 (1993).

17. J.M. Watson, I. NoorBatcha, and R.R. Lucchese, J.Chem.Phys. **96**, 7771 (1992).

18. V.J. Barclay, D.B. Jack, J.C. Polanyi, and Y. Zeiri, J.Chem.Phys. **97**, 9458 (1992).

19. a) H. Guo and G.C. Schatz, Chem.Phys.Lett. **184**, 245 (1991); b) *ibid*, J.Chem.Phys. **94**, 379 (1991).

20. M.I. McCarthy, R.B. Gerber, and M. Shapiro, J.Chem.Phys. **92**, 7708 (1990).

21. M.S. Slutsky and T.F. George, Chem.Phys.Lett. **57**, 474 (1978).

22. P.M. Blass, R.C. Jackson, J.C. Polanyi, and H. Weiss, J.Chem.Phys. **94**, 7003 (1991).

23. J.C. Polanyi, R.J. Williams, and S.F. O'Shea, J.Chem.Phys. **94**, 978 (1991).

24. T. Seideman, J.Chem.Phys. **98**, 1989 (1993).

25. a) D.A. Chapman, K. Balasubramanian, and S.H. Lin, Chem.Phys. **118**, 333 (1987); b) D.A. Chapman, private communication.

26. L.C. Lee and M. Suto, Proc. SPIE **911** *X-Ray and Vacuum Ultraviolet Interaction Data Bases, Calculations, and Measurements*, p. 39 (1988).

27. R.S. Mulliken, J.Chem.Phys. **8**, 382 (1940).

28. Z. Xu, B. Koplitz, and C. Wittig, J.Phys.Chem. **92**, 5518 (1988).

29. J.E. Lennard-Jones and B.M. Dent, Trans.Faraday.Soc. **24**, 92 (1928).

30. W.A. Steele, *The Interaction of Gases with Solid Surfaces*, (Pregamon Press, New York, 1974).

31. A.J. Stone and M. Alderton, Molec.Phys. **56**, 1047 (1985).

32. R.D Levine, *Quantum Mechanics of Molecular Rate Processes* (Clarendon, Oxford, 1969).

33. The name Lippmann-Schwinger usually refers to the equivalent formal expression for the scattering state in terms of a zero order Green's operator and the exact wavefunction. See, for example, Ref. 32 Eq. (2.1.11)

34. R. Kosloff and D. Kosloff, J.Comput.Phys. **63**, 363 (1986); D. Neuhauser and M. Baer, J.Chem.Phys. **90**, 4351 (1989); T. Seideman and W.H. Miller, J.Chem.Phys. **96**, 4412 (1992); *ibid* **97**, 2499 (1992).

35. for a review see J.C. Light, R.M. Whitnell, T.J. Park, and S.E. Choi, in *Supercomputer Algorithms for Reactivity, Dynamics and Kinetics of Small Molecules*, A. Lagana Ed., NATO ASI Series C, Vol. 277, p. 187 (1989).

36. M. Abramowitz and I.A. Stegun, *Handbook of Mathematical Functions* (Dover, New-York, 1965).

37. a) J.D. Doren and J.C. Tully, Langmuir 4 256, (1988); b) N. Makri and W.H. Miller, J.Chem.Phys. **87**, 5781 (1987); c) K. Haug and H. Metiu, J.Chem.Phys. **97**, 4781 (1992).

38. See, for example, D. Chandler and L.R. Pratt, J.Chem.Phys. **65**, 2925 (1976); E. Pollak, J.Chem.Phys. **95**, 533 (1991).

Figure Captions

1. Schematic illustration of HBr adsorbed on a LiF surface following the IR measurements of Ref. 22.

2. Potential energy curves for HBr (derived from Ref. 25).

3. Substrate-adsorbate interaction as a function of the Cartesian coordinates of the H atom. z' denotes height above the surface and x denotes distance along the [100] crystallographic axis with Li^+ defining the origin. The Br atom is fixed at its equilibrium position.
   (a) for bound (molecular) HBr
   (b) for free (atomic) H+Br.
   Contours are in increments of 1eV.

4. Total photodissociation cross section for HBr as a function of the photon wavelength:
   (- - - - - -) gas phase HBr
   (————) surface adsorbed HBr.

5. Angular distribution $\sigma(\theta_k, \lambda = 193 \text{ nm})$ of the hydrogen photofragments corresponding to the $Br(^2P_{3/2})$ channel following excitation of HBr/LiF(001) at 193 nm. θ_k is measured with respect to the surface normal.

6. Experimental angular distributions of the hydrogen photofragment corresponding to the $Br(^2P_{3/2})$ channel at different surface coverages:
   (o o o o) 0.2 monolayer
   (• • • •) 0.5 monolayer
   (□ □ □ □) 1.0 monolayer.
   (Reproduced from Ref. 9 with permission of the authors.)

7. Angular distribution of the H photofragments following excitation at 193 nm:
   (————) light polarized along the z axis
   (- - - - -) light polarized along the x axis.

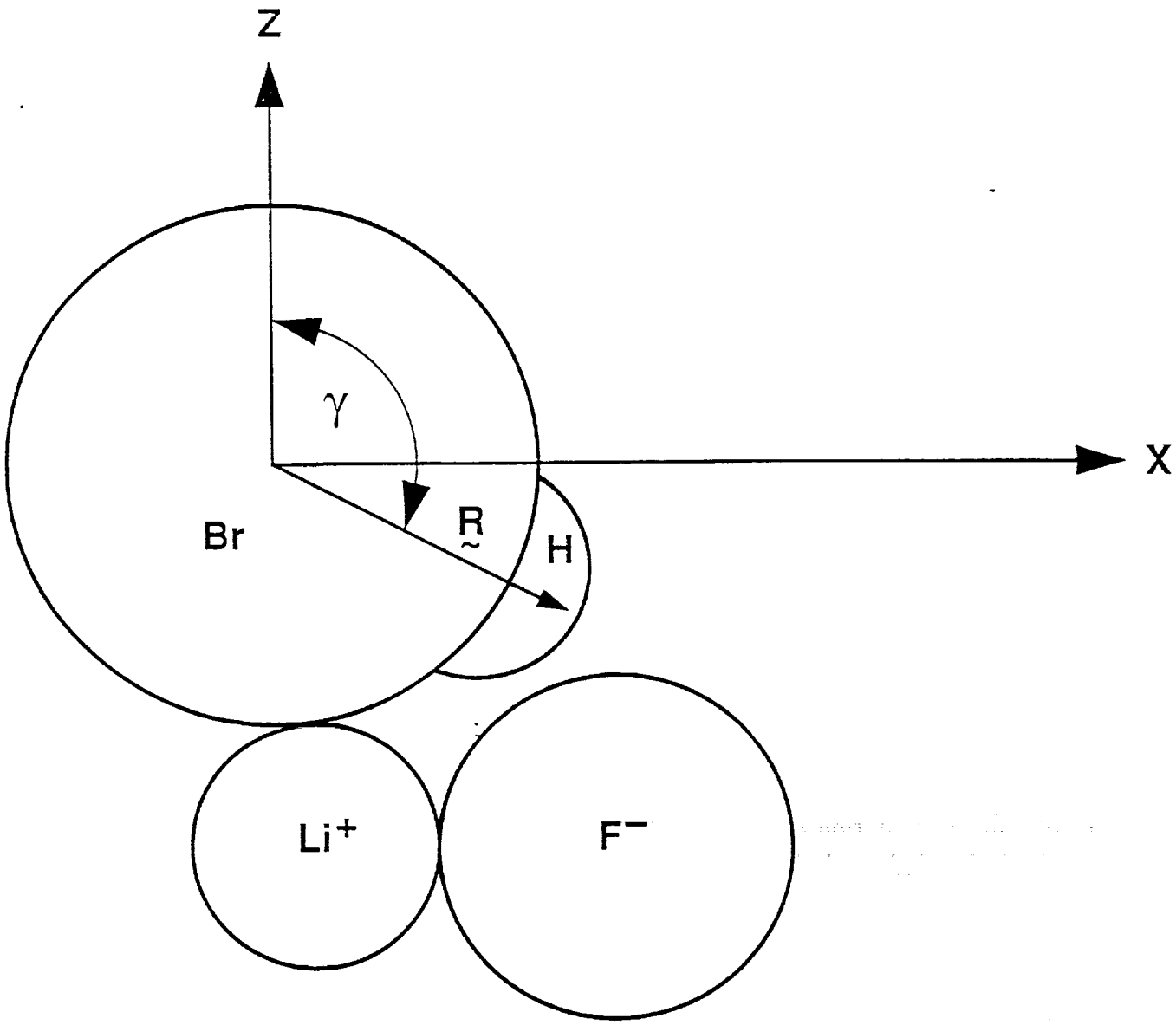

Seideman-1

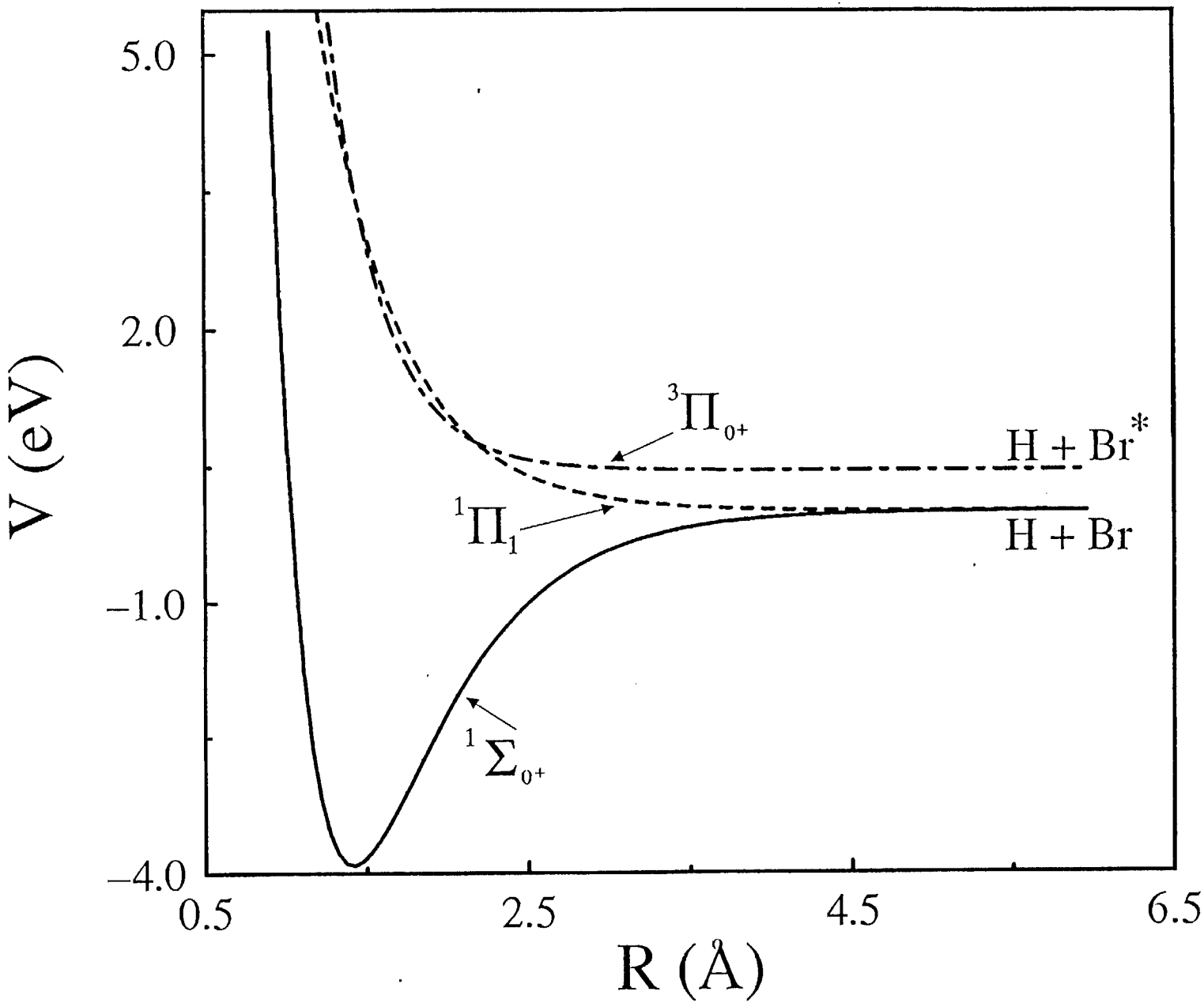
5.0
2.0
−1.0
−4.0
V (eV)
0.5
2.5
4.5
6.5
R (Å)
$^3\Pi_{0^+}$
$^1\Pi_1$
$^1\Sigma_{0^+}$
H + Br*
H + Br

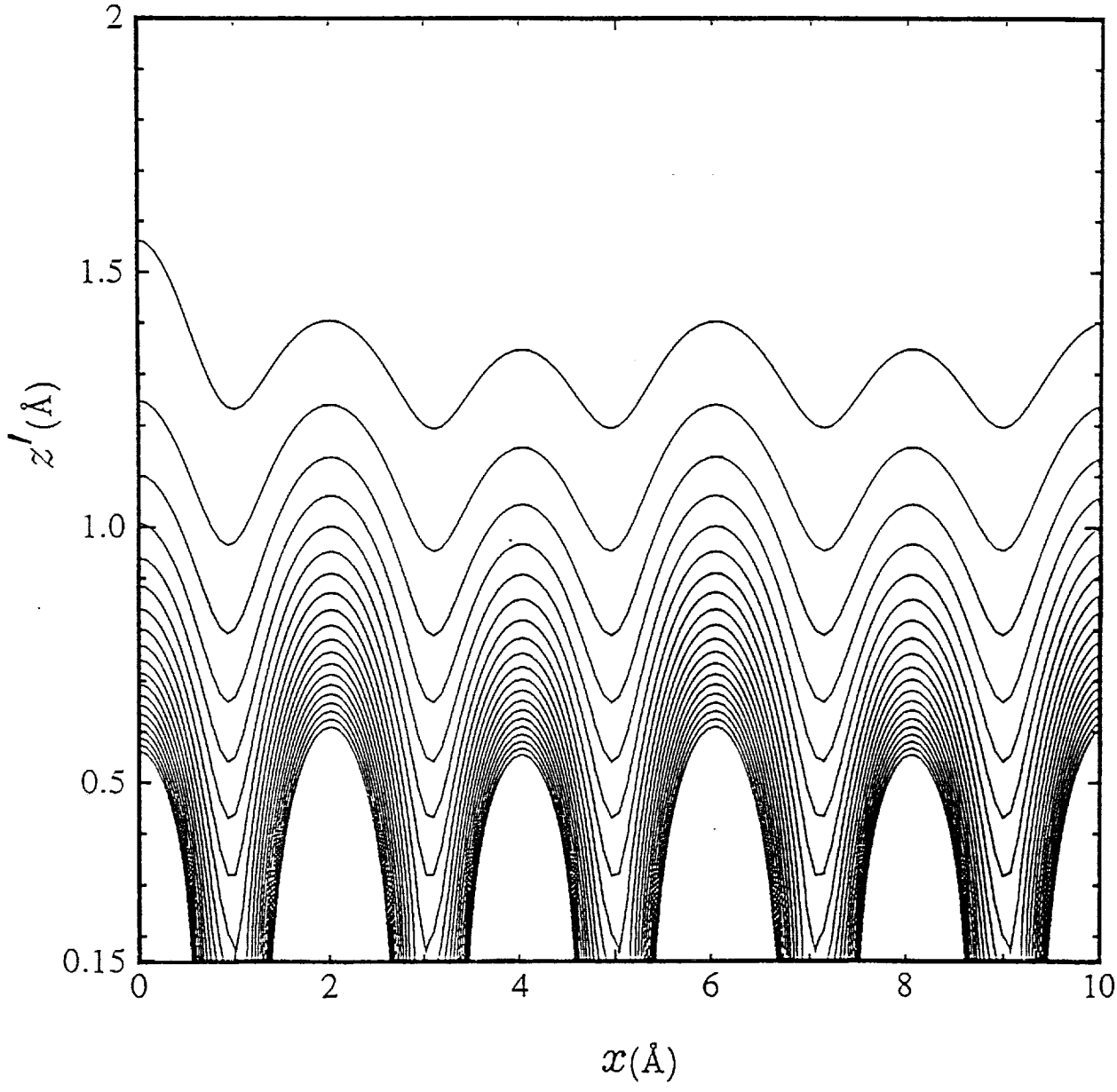
2
1.5
1.0
0.5
0.15
z'(Å)
0
2
4
6
8
10
x(Å)

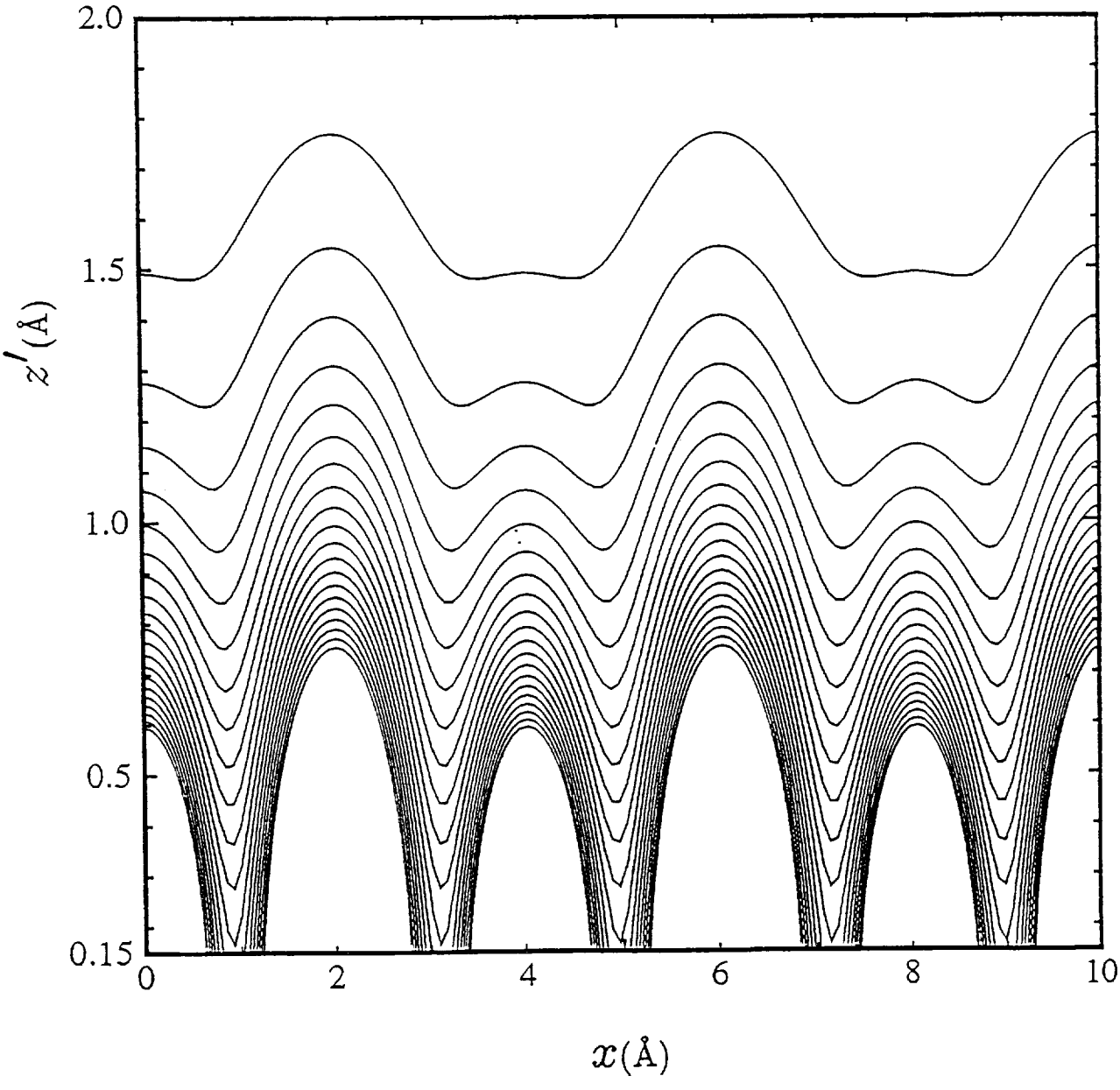
2.0
1.5
1.0
0.5
0.15
z'(Å)
0
2
4
6
8
10
x(Å)

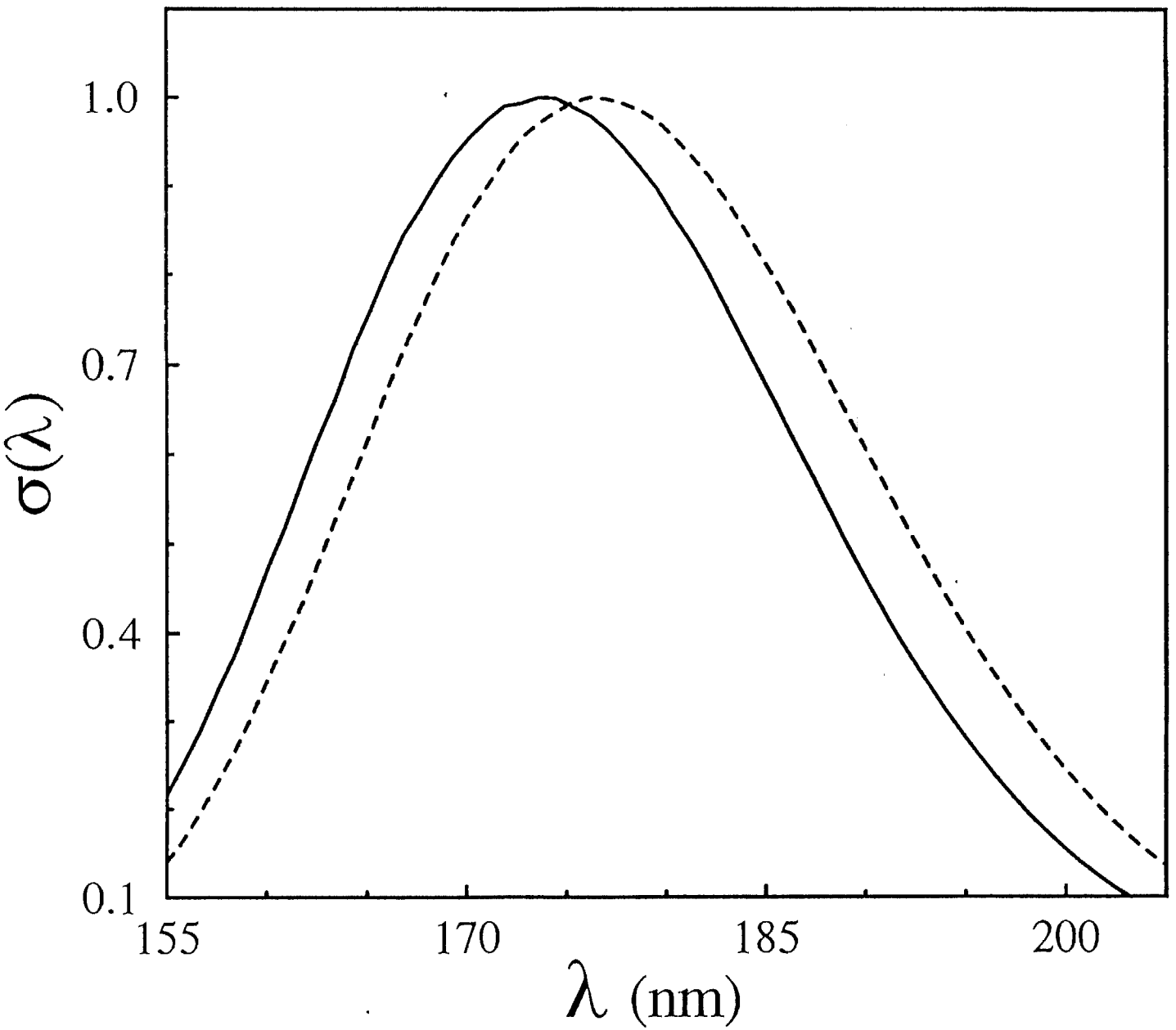
1.0
0.7
0.4
0.1
σ(λ)
155
170
185
200
λ (nm)

σ(θk)
0.0
0.3
0.6
0.9
20
40
60
80
θk (deg)

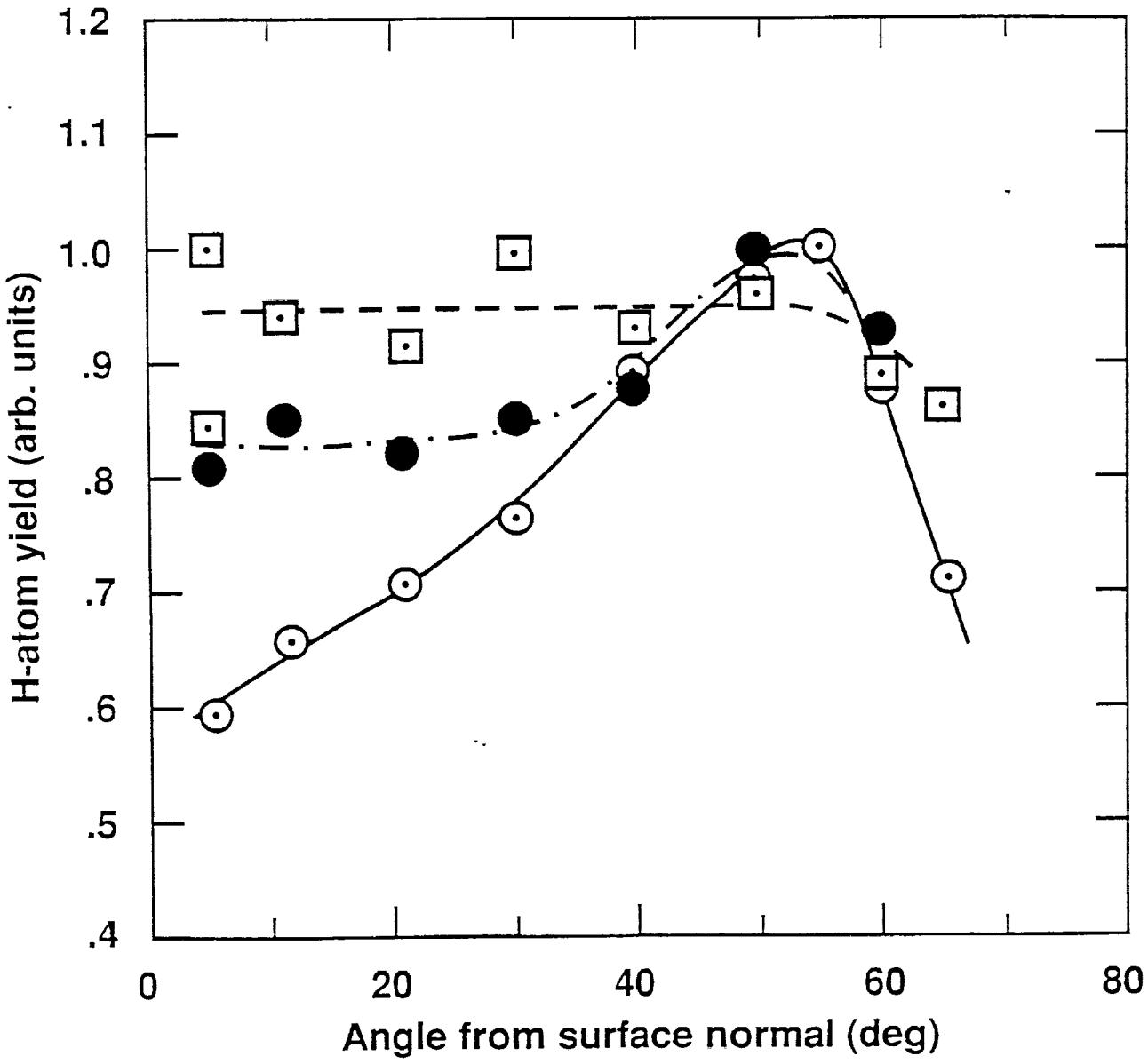
1.2
1.1
1.0
.9
.8
.7
.6
.5
.4
H-atom yield (arb. units)
0
20
40
60
80
Angle from surface normal (deg)

Seideman-1

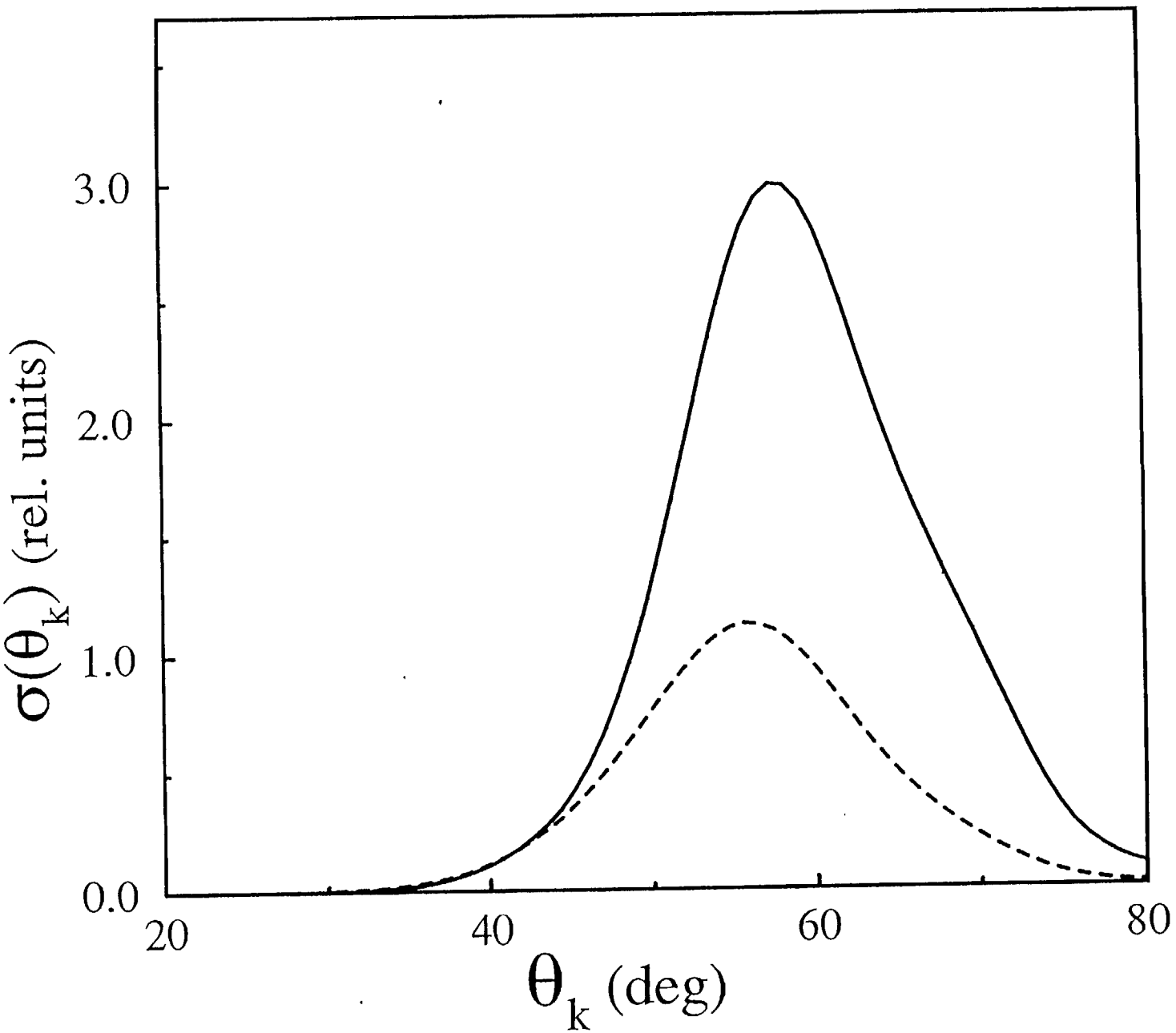
3.0
2.0
1.0
0.0
$\sigma(\theta_k)$ (rel. units)
20
40
60
80
θ_k (deg)